JOURNAL OF VIROLOGY, Aug. 2007, p. 8821–8826 Vol. 81, No. 16
0022-538X/07/$08.00+0 doi:10.1128/JVI.00754-07

Reversible Inhibition of the Fusion Activity of Measles Virus F Protein by an Engineered Intersubunit Disulfide Bridge▽

Jin K. Lee,[1] Andrew Prussia,[2] James P. Snyder,[2] and Richard K. Plemper[1]*

Department of Pediatrics, Emory University School of Medicine, Atlanta, Georgia 30322,[1] and Department of Chemistry, Emory University, Atlanta, Georgia 30322[2]

Received 7 April 2007/Accepted 25 May 2007

In search of target sites for the development of paramyxovirus inhibitors, we have engineered disulfide bridges to introduce covalent links into the prefusion F protein trimer of measles virus. F-Edm-452C/460C, predicted to bridge head and stalk domains of different F monomers, shows a high degree of proteolytic maturation and surface expression, predominantly as stable, dithiothreitol-sensitive trimers, but no fusion activity. Reduction of disulfide bridges partially restores activity. These findings underscore the importance of reversible intersubunit interactions between the stalk and head domains for F activity. Noncovalent small molecules mimicking this behavior may constitute a potent strategy for preventing paramyxovirus entry.

Measles virus (MV), a paramyxovirus, accounts for approximately 25 million cases and 400,000 deaths annually (2, 27). Blocking entry of enveloped viruses has proven to be an efficacious therapeutic strategy (9, 23). The paramyxovirus fusion (F) protein trimer mediates fusion of the viral envelope with the target cell plasma membrane (6, 13, 22). Through structure-based drug design, we previously developed a small-molecule MV entry inhibitor, AS-48 (17, 25), that stabilizes a conformational intermediate transiently emerging during refolding of F from the pre- to postfusion state (5). However, targeting a site present in prefusion F may constitute a superior intervention strategy.

Crystallization of prefusion F of parainfluenzavirus 5 (PIV5), a paramyxovirus related to MV, has advanced the mechanistic understanding of F activity (28). Instrumental in the process are, among others, two heptad repeat domains (HR-A and HR-B), which ultimately assemble into a six-helix bundle structure (7, 21). In prefusion F, a globular head is postulated to engage at its base in reversible intersubunit interactions with residues at the top of a triple-helix stalk formed by the HR-B domains (21, 28). This head includes the HR-A domains, broken up into distinct segments (28). Transition from the pre- to postfusion conformation is proposed to require melting of the HR-B stalk and movement of the HR-B domains around the base of the head to interact with a triple-helix HR-A stalk assembled from its prefusion segments (4, 28).

In search of a candidate target for antivirals in prefusion F, we hypothesize that fusion may be blocked by stabilizing noncovalent interactions in the prefusion F head or between the head and stalk of different subunits. To obtain proof of concept, we have examined whether disulfide bridges, engineered to covalently link these microdomains, can arrest fusion.

Molecular modeling of disulfide bonds in prefusion MV F. Based on the coordinates reported for prefusion PIV5 F, we generated a structural model of prefusion MV F. Following sequence alignment using Clustal W (3), the homology model was constructed with Prime (Schrödinger) and refined using Prime's side-chain prediction protocol. The model was analyzed in silico using Sybyl 7.0 (Tripos) and the Lovell rotamer library (15) to identify residues in the targeted domains with the potential to form disulfide bonds when mutated pairwise to cysteine, without necessitating large-scale domain movements.

An intersubunit disulfide bond between residues 452 and 460 (Ile452 and Gly460 in unmodified MV F), postulated to link the base of the head to the prefusion stalk (Fig. 1A, B, and C), and an intrasubunit bond between residues 307 and 448 (Gly307 and Leu448 in unmodified MV F), postulated to link adjacent loops in the head domain (Fig. 1D, E, and F), appeared promising based on their side-chain geometries. All of these residues are highly conserved among F proteins derived from different MV genotypes and other members of the morbillivirus genus (canine distemper virus [strains examined, Onderstepoort and Lederle]) and rinderpest virus (strains examined, RBOK and Kabete O). Both centers were treated to mutation, bond formation, and refinement by short, 20,000-molecular-weight (20K) molecular dynamics runs using Macromodel 9.4 (Schrödinger) and force field minimization using OPLS2005 (10–12) and GB/SA solvation (24). The bonds between residues 452 and 460 and 307 and 448 display x_3 angles of −103.1 and 90.8°, respectively. While both angles are close to the ideal, the bond between residues 307 and 448 perturbs the original structure slightly more than the bond between residues 452 and 460. The root mean square deviations between the backbone atoms within an 8 Å sphere around the bonds is 0.73 Å for the bond between residues 452C and 460C and 1.43 Å for the bond between residues 307C and 448C. Thus, formation of the disulfide bond between residues 452 and 460 was predicted to be slightly more favorable.

Expression and fusion activity of F mutants with engineered disulfide bonds. Pairwise changes to cysteines were realized in expression plasmids carrying the F gene of the MV-Edmonston (MV-Edm) vaccine strain under control of the cytomegalo-

* Corresponding author. Mailing address: Division of Infectious Diseases, Department of Pediatrics, 520 Children's Center, 2015 Uppergate Drive, Emory University School of Medicine, Atlanta, GA 30322. Phone: (404) 727-1605. Fax: (404) 727-9223. E-mail: rplempe@emory.edu.

▽ Published ahead of print on 6 June 2007.

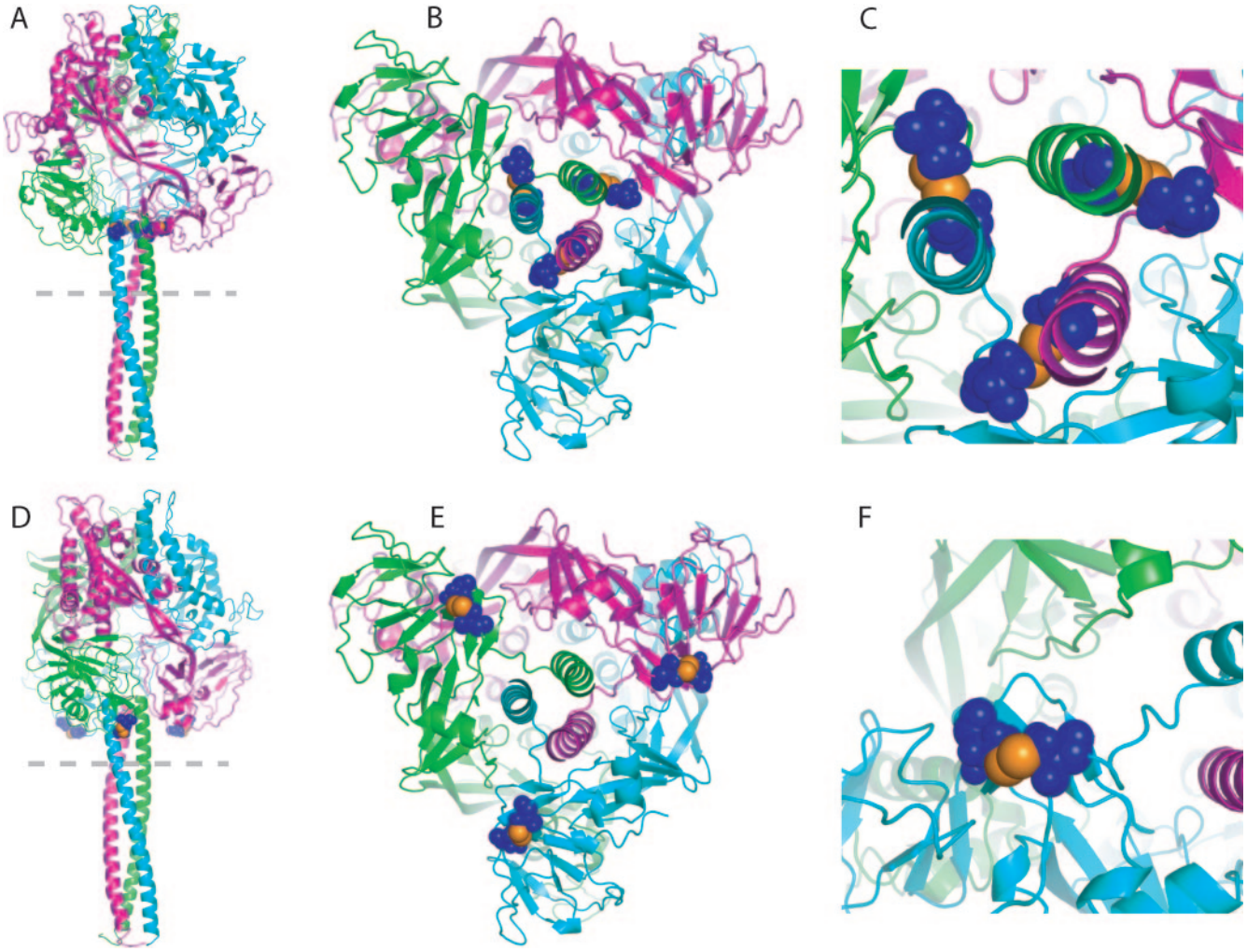

FIG. 1. Predicted geometries of disulfide bonds introduced into the prefusion MV F trimer. Homology models of MV F were generated on the basis of the coordinates reported for prefusion PIV5 F and are colored by monomer subunits. (A, B, and C) A disulfide bond between residues 452 and 460 is predicted to establish an intersubunit link between the top of the HR-B prefusion stalk and the base of the globular head domain. Side view of the trimer (A), view from the dotted line in panel A up the HR-B stalk (B), and close-up view of the intersection of stalk and head domain (C). Cysteine side chains of engineered bonds are highlighted in blue; individual sulfur atoms are shown in orange. (D, E, and F) A disulfide bond between residues 307 and 448 is predicted to link two loops in the base of the prefusion head domain of the same monomer. Individual views and coloring of engineered bonds as described for panels A through C.

virus promoter (1). Following site-directed mutagenesis (QuikChange; Stratagene) and confirmation by DNA sequencing, both variants and the unmodified parent plasmid were transfected in Vero cells. F expression was examined by precipitation from cleared cell lysates using an antiserum against residues 127 to 193 in the HR-A domain. This serum recognizes both membrane-embedded native F and F in cell lysates. Following separation under reducing conditions, precipitated F was detected through immunostaining using antibodies against its cytosolic tail. F-Edm-452C/460C showed efficient proteolytic maturation of the F_0 precursor (Fig. 2A). In contrast, no maturation was detected for F-Edm-307C/448C, suggesting its misfolding and likely intracellular retention (Fig. 2A).

This was assessed by surface biotinylation to determine plasma membrane steady-state levels. Biotinylated proteins were precipitated using immobilized streptavidin, and surface-expressed F was immunoblotted and quantified using a VersaDoc imaging system (Bio-Rad). F-Edm-452C/460C largely maintained intracellular transport competence, showing a surface steady-state level of approximately 70% of unmodified F-Edm, whereas F-Edm-307C/448C was virtually undetectable at the cell surface (Fig. 2B).

To assess fusion activity of the mutants, we employed a quantitative cell-to-cell fusion assay. Effector cells, transfected with plasmids encoding MV-H and the F construct of interest and infected with modified vaccinia virus Ankara expressing T7 polymerase (26), were overlaid 14 h posttransfection with target cells containing a luciferase reporter under the control of the T7 promoter. Luciferase activity in cell lysates was determined 200 min postoverlay using a luminescence counter (PerkinElmer). Both F variants failed to induce cell-to-cell fusion (Fig. 2C), also confirmed by microscopic examination (see Fig. 4A for F-Edm-452C/460C; data not shown for F-Edm-307C/448C). While this was expected for F-Edm-307C/

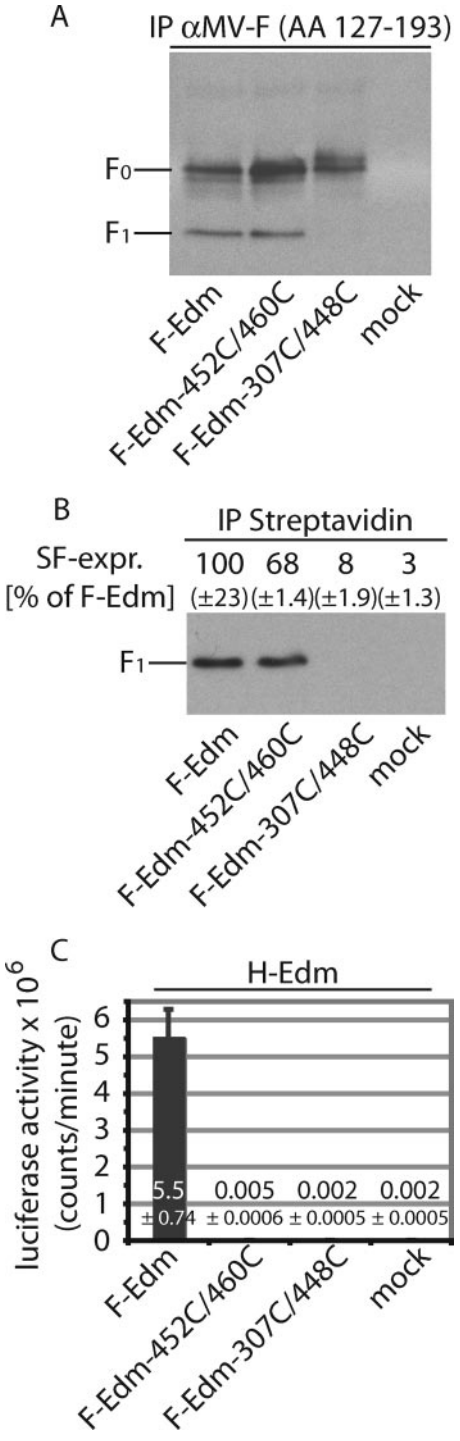

FIG. 2. An F-Edm-452C/460C double mutant is proteolytically activated and intracellular transport competent but lacks fusion activity. (A) Immunoprecipitation (IP) of F-Edm, F-Edm-452C/460C, and F-Edm-307C/448C from cleared Vero cell lysates obtained 36 h posttransfection. An antiserum directed against residues 127 to 193 in the F HR-A domain was employed. Precipitated material was subsequently subjected to immunostaining using antibodies directed against the cytosolic F tail as previously described (19). Both the F_0 precursor and the proteolytically matured F_1 fraction of F-Edm and F-Edm-452C/460C are present, while for F-Edm-307C/448C, only the uncleaved F_0 precursor is visible. Samples were fractionated under reducing conditions, mock-transfected cells did not express any MV F antigenic material, and immunoblots were decorated with rabbit immunoglobulin G light-chain-specific horseradish peroxidase conjugate. (B) The F-Edm-452C/460C mutant but not F-Edm-307C/448C is expressed at the cell surface. Surface biotinylation to assess plasma membrane steady-state levels of MV F was carried out as described previously (16). Values above the blot are based on densitometric quantification of signal intensities using a VersaDoc imaging station. Averages of the results of two independent experiments and standard error of the mean values are presented. (C) Quantitative cell-to-cell fusion assays reveal that both F-Edm variants lack fusion activity. Effector Vero cells were infected with MVA-T7 and cotransfected with 3 μg plasmid DNA, each encoding H-Edm or the F construct specified. Target cells harbored a luciferase reporter construct under the control of the T7 promoter, and luciferase activities as an indicator of cell-to-cell fusion activity were assessed 200 min postmixing of both populations. Mock effector cells received only MVA-T7 and H-Edm encoding plasmid. Bar graphs and numbers show averages and standard deviation values of the results of three independent experiments.

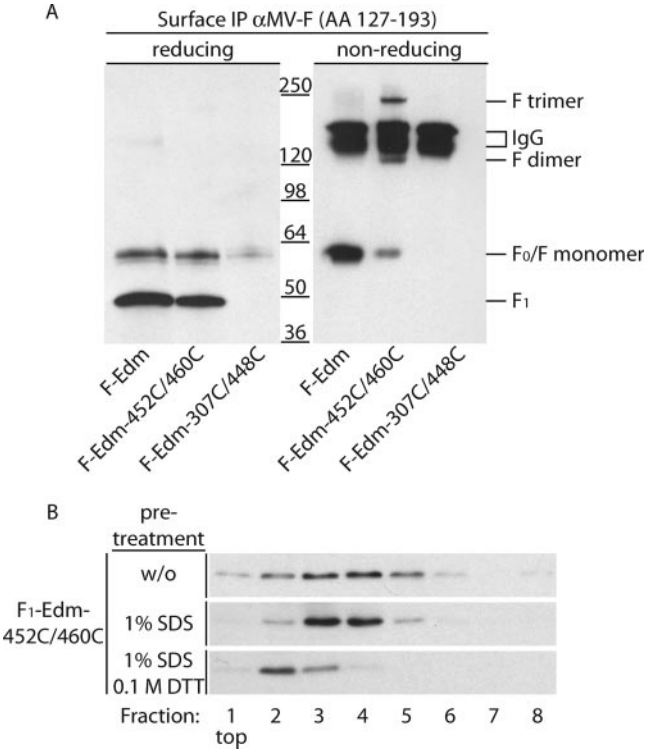

FIG. 3. Disruption of F-Edm-452C/460C trimers requires reducing conditions, indicating presence of intersubunit disulfide bonds. (A) Surface immunoprecipitation (IP) of F-Edm, F-Edm-452C/460C, and F-Edm-307C/448C using an antiserum directed against the HR-A domain, followed by gel electrophoresis under reducing (in the presence of 1.5% DTT) and nonreducing (in the absence of DTT) conditions and immunodetection with F-tail-specific antibodies. Under nonreducing conditions, the majority of the F-Edm-452C/460C antigenic material migrates as trimer, while parental F-Edm migrates exclusively as monomer. Reduction of disulfide bonds through DTT treatment results in migration of the majority of F-Edm and F-Edm-452C/460C antigenic material as F_1 monomers. Immunoblots were decorated with rabbit immunoglobulin G light-chain-specific horseradish peroxidase conjugate. (B) Fractionation of cell lysates harboring F-Edm-452C/460C on 10 to 25% sucrose gradients, carried out essentially as described previously (14, 18). Prior to loading on gradients, each lysate was treated for 30 min with 1% SDS or 1% SDS and 0.1 M DTT or left untreated (w/o). The gradient fractions were subjected to trichloroacetic acid precipitation, followed by gel electrophoresis under reducing conditions. No redistribution of the F-Edm-452C/460C material to a lower density fraction occurs upon treatment with SDS alone.

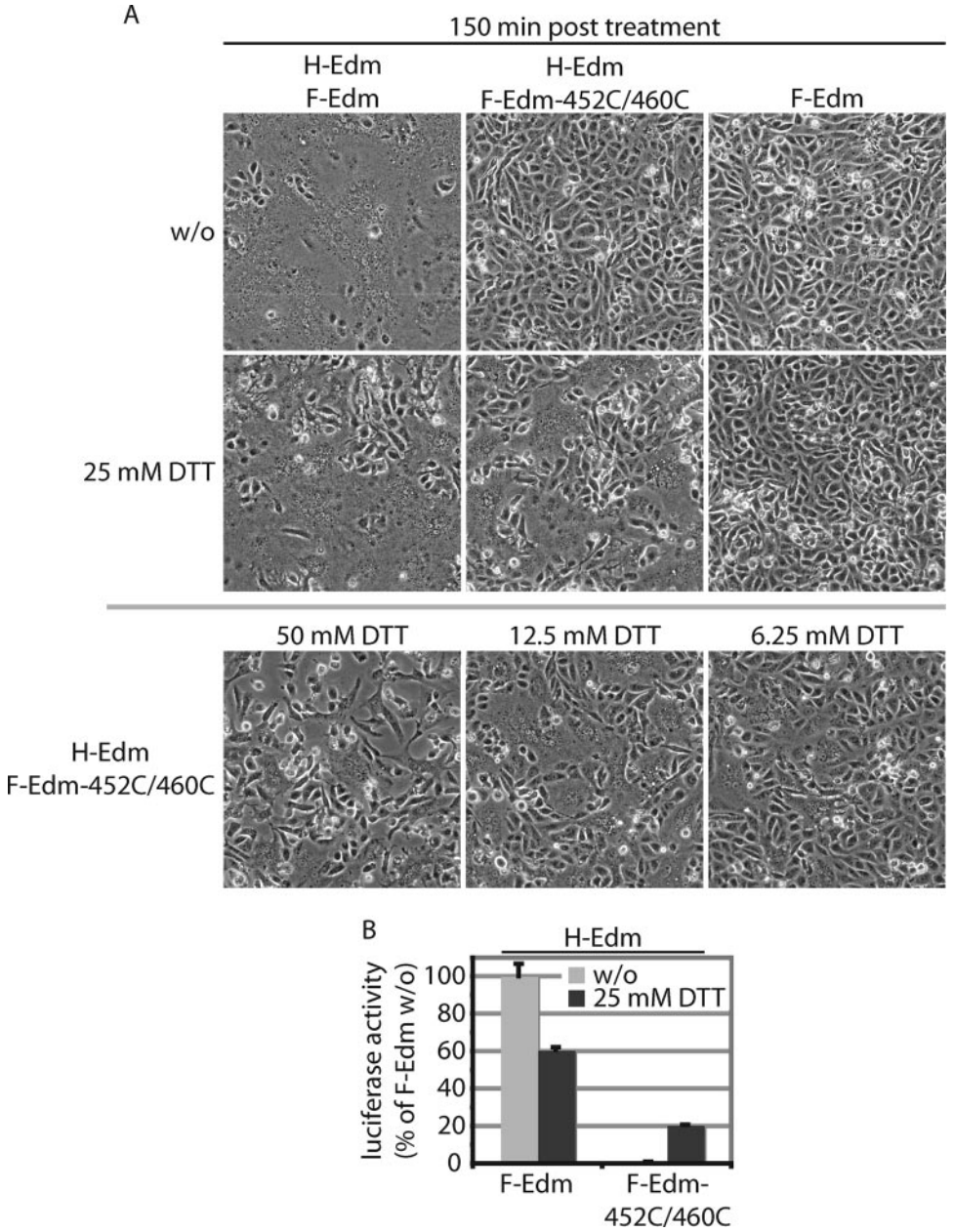

FIG. 4. DTT treatment of cells coexpressing H-Edm and F-Edm-452C/460C results in partial reactivation of F-Edm-452C/460C fusion activity. (A) (Top two rows) microphotographs of Vero cells cotransfected with 3 μg plasmid DNA each encoding H-Edm or F-Edm, or encoding H-Edm or F-Edm-452C/460C, or transfected with F-Edm encoding plasmids alone. Thirty hours posttransfection, cells were treated with DTT or left untreated (w/o), followed by an iodoacetamide wash and microscopic assessment of fusion activity 150 min posttreatment. F-Edm-452C/460C-expressing cells formed syncytia only after treatment with DTT. Prior to the time of DTT treatment, H-Edm/F-Edm-expressing cells were kept in the presence of fusion inhibitory peptide (Bachem) to prevent premature syncytia formation. (Bottom row) cells cotransfected with H-Edm and F-Edm-452C/460C as described above but treated with 6.25, 12.5, or 50 mM DTT for 150 min for comparison. The most substantial activation of F-Edm-452C/460C occurs when cells were treated with 12.5 or 25 mM DTT. All microphotographs were taken at a magnification of ×200. (B) Quantification of fusion activity of cells transfected as in panel A using the luciferase reporter assay outlined in Fig. 2C. While treatment with 25 mM DTT reduces fusion activity of F-Edm by approximately 40% compared to untreated (w/o) H-Edm/F-Edm-expressing cells, it restores activity of F-Edm-452C/460C to levels corresponding to 20% of untreated F-Edm. No fusion activity was detected in untreated cells expressing H-Edm and F-Edm-452C/460C. Luciferase activities were normalized for values obtained for untreated, H-Edm/F-Edm-expressing cells. Averages and standard error of the mean values are shown.

448C, considering its lack of transport competence, the absence of fusion activity of proteolytically cleaved and surface-expressed F-Edm-452C/460C provided first evidence for successful intersubunit disulfide bond formation.

Oligomerization of F variants with engineered disulfide bonds. To test the oligomerization status of cell surface F-Edm-452C/460C, surface immunoprecipitation was carried out using the HR-A-specific antiserum. Samples were sepa-

rated under reducing and nonreducing conditions, and F was detected by immunoblotting as described above. Intracellularly retained F-Edm-307C/448C was included as control.

Under reducing conditions, the majority of F-Edm and F-Edm-452C/460C migrated at a molecular weight corresponding to proteolytically cleaved F_1 (Fig. 3A), confirming our initial observations. Under nonreducing conditions, the majority of F-Edm-452C/460C migrated at a molecular weight corresponding to F trimers, with only small amounts of dimeric and monomeric material detected (Fig. 3A). In contrast, noncovalently linked F-Edm trimers disintegrated and migrated exclusively as F monomers.

Stability of F-Edm-452C/460C oligomers was further assessed using sucrose velocity gradient centrifugation. Lysates of cells expressing F-Edm-452C/460C were incubated in the presence of 1% Triton X-100, 1% sodium dodecyl suflate (SDS), or 1% SDS and 0.1 M dithiothreitol (DTT) for 30 min at 25°C, fractionated on 10 to 25% sucrose gradients, and F detected in trichloroacetic acid precipitates of individual fractions by immunoblotting using F-tail-specific antibodies. SDS treatment alone, which disrupts noncovalent protein-protein interactions in the MV F trimer (18), had little effect on the distribution of F-Edm-452C/460C in the gradient (Fig. 3B; the majority of F antigenic material is present in fractions 3 and 4). In contrast, the majority of higher-molecular-weight material shifted to lower-density fractions (fraction 2) upon reduction of covalent disulfide bonds by DTT.

These results indicate that covalent, DTT-sensitive, intersubunit bonds are present in the majority of F-Edm-452C/460C trimers.

Reactivation of fusion activity by DTT treatment. To test whether partial reduction of disulfide bonds results in reactivation of F-Edm-452C/460C fusion activity, cells coexpressing this mutant and H-Edm were treated for 30 min with concentrations of DTT ranging from 50 to 6.25 mM, followed by acetylation of thiol groups with 1 mM iodoacetamide as described previously (8) and microscopic assessment of fusion activity after 150 min. The greatest reactivation of F-Edm-452C/460C fusion was found upon treatment with 12.5 or 25 mM DTT (Fig. 4A), while higher concentrations appeared increasingly harmful to target cells. Following treatment, multinucleated cells (syncytia) indicating cell-to-cell fusion formed, while no syncytia appeared in untreated controls. Furthermore, assessment of cells coexpressing H-Edm and F-Edm revealed that DTT treatment reduces fusion somewhat (Fig. 4A), presumably through reduction of natural disulfide bonds in the viral glycoproteins.

Fusion activity was quantified using the luciferase-reporter cell-to-cell fusion assay. Cells expressing H-Edm/F-Edm-452C/460C and treated with 25 mM DTT, the highest concentration tolerated by the cells without visible signs of cytotoxicity, showed fusion at 20% that of untreated cells expressing H-Edm/F-Edm (Fig. 4B). In contrast, treatment reduced fusion activity of H-Edm/F-Edm-expressing cells to 60% of untreated controls. This equals an approximately fourfold increase in relative luciferase units for F-Edm-452C/460C upon DTT treatment compared to a 1.6-fold reduction upon treatment for F-Edm. These findings indicate proper folding and reversible covalent fixation of F-Edm-452C/460C trimers in a prefusion conformation.

In summary, our study demonstrates that a disulfide bond can be successfully engineered between residues of separate paramyxovirus F monomers that are predicted to be located at the intersection of the prefusion F head and stalk domains. According to our structural model, mutating residues 452 and 460 to cysteines results in a high propensity for intersubunit disulfide bond formation, while a bond between residues 307C and 448C is slightly less favorable. The experimental findings are consistent with these predictions, lending support to the validity of our homology model of prefusion MV F.

Introduction of an intersubunit disulfide bond at the intersection of prefusion F head and stalk domains abolishes fusion, and its reduction partially restores fusion activity. This demonstrates that reversible noncovalent intersubunit interactions at the contact zone of both domains play an important role in the fusion process. Our findings are consistent with the observation that mutation of residues involved in these interactions destabilizes the metastable prefusion conformation of F (20, 28). They furthermore implicate the contact zone of prefusion head and stalk as a promising target for structure-based drug development. An ideal inhibitor will dock into this zone and, by means of forces such as hydrogen bonds, pi-cation interactions, and hydrophobic effects, stabilize the interaction between both domains. A corresponding increase in the energy barrier for activation of metastable prefusion F would mimic the fusion-silencing effect of the engineered disulfide bond.

We thank A. L. Hammond for comments on the manuscript.

This work was supported by the American Lung Association and Public Health Service grants AI056179 and AI071002 from NIH/NIAID (to R.K.P.).

REFERENCES

1. **Cathomen, T., H. Y. Naim, and R. Cattaneo.** 1998. Measles viruses with altered envelope protein cytoplasmic tails gain cell fusion competence. J. Virol. **72:**1224–1234.
2. **Centers for Disease Control and Prevention.** 2005. Progress in reducing measles mortality—worldwide, 1999–2003. Morb. Mortal. Wkly. Rep. **54:** 200–203.
3. **Chenna, R., H. Sugawara, T. Koike, R. Lopez, T. J. Gibson, D. G. Higgins, and J. D. Thompson.** 2003. Multiple sequence alignment with the Clustal series of programs. Nucleic Acids Res. **31:**3497–3500.
4. **Connolly, S. A., G. P. Leser, H. S. Yin, T. S. Jardetzky, and R. A. Lamb.** 2006. Refolding of a paramyxovirus F protein from prefusion to postfusion conformations observed by liposome binding and electron microscopy. Proc. Natl. Acad. Sci. USA **103:**17903–17908.
5. **Doyle, J., A. Prussia, L. K. White, A. Sun, D. C. Liotta, J. P. Snyder, R. W. Compans, and R. K. Plemper.** 2006. Two domains that control prefusion stability and transport competence of the measles virus fusion protein. J. Virol. **80:**1524–1536.
6. **Dutch, R. E., T. S. Jardetzky, and R. A. Lamb.** 2000. Virus membrane fusion proteins: biological machines that undergo a metamorphosis. Biosci. Rep. **20:**597–612.
7. **Eckert, D. M., and P. S. Kim.** 2001. Mechanisms of viral membrane fusion and its inhibition. Annu. Rev. Biochem. **70:**777–810.
8. **Godley, L., J. Pfeifer, D. Steinhauer, B. Ely, G. Shaw, R. Kaufmann, E. Suchanek, C. Pabo, J. J. Skehel, D. C. Wiley, et al.** 1992. Introduction of intersubunit disulfide bonds in the membrane-distal region of the influenza hemagglutinin abolishes membrane fusion activity. Cell **68:**635–645.
9. **Greenberg, M., N. Cammack, M. Salgo, and L. Smiley.** 2004. HIV fusion and its inhibition in antiretroviral therapy. Rev. Med. Virol. **14:**321–337.
10. **Jorgensen, W. L., and J. Tiradorives.** 1988. The OPLS potential functions for proteins—energy minimizations for crystals of cyclic-peptides and crambin. J. Am. Chem. Soc. **110:**1657–1666.
11. **Kaminski, G., E. M. Duffy, T. Matsui, and W. L. Jorgensen.** 1994. Free energies of hydration and pure liquid properties of hydrocarbons from the OPLS all-atom model. J. Phys. Chem. **98:**13077–13082.
12. **Kaminski, G. A., R. A. Friesner, J. Tirado-Rives, and W. L. Jorgensen.** 2001. Evaluation and reparametrization of the OPLS-AA force field for proteins via comparison with accurate quantum chemical calculations on peptides. J. Phys. Chem. B. **105:**6474–6487.
13. **Lamb, R. A., and D. Kolakofsky.** 2001. Paramyxoviridae: the viruses and their

replication, p. 1305–1340. *In* D. M. Knipe and P. M. Howley (ed.), Fields virology, 4th ed. Lippincott Williams & Wilkins, Philadelphia, PA.
14. **Loe, D. W., K. C. Almquist, R. G. Deeley, and S. P. Cole.** 1996. Multidrug resistance protein (MRP)-mediated transport of leukotriene C4 and chemotherapeutic agents in membrane vesicles. Demonstration of glutathione-dependent vincristine transport. J. Biol. Chem. **271:**9675–9682.
15. **Lovell, S. C., J. M. Word, J. S. Richardson, and D. C. Richardson.** 2000. The penultimate rotamer library. Proteins **40:**389–408.
16. **Plemper, R. K., and R. W. Compans.** 2003. Mutations in the putative HR-C region of the measles virus F_2 glycoprotein modulate syncytium formation. J. Virol. **77:**4181–4190.
17. **Plemper, R. K., J. Doyle, A. Sun, A. Prussia, L. T. Cheng, P. A. Rota, D. C. Liotta, J. P. Snyder, and R. W. Compans.** 2005. Design of a small-molecule entry inhibitor with activity against primary measles virus strains. Antimicrob. Agents Chemother. **49:**3755–3761.
18. **Plemper, R. K., A. L. Hammond, and R. Cattaneo.** 2001. Measles virus envelope glycoproteins hetero-oligomerize in the endoplasmic reticulum. J. Biol. Chem. **276:**44239–44246.
19. **Plemper, R. K., A. L. Hammond, D. Gerlier, A. K. Fielding, and R. Cattaneo.** 2002. Strength of envelope protein interaction modulates cytopathicity of measles virus. J. Virol. **76:**5051–5061.
20. **Russell, C. J., K. L. Kantor, T. S. Jardetzky, and R. A. Lamb.** 2003. A dual-functional paramyxovirus F protein regulatory switch segment: activation and membrane fusion. J. Cell Biol. **163:**363–374.
21. **Russell, C. J., and L. E. Luque.** 2006. The structural basis of paramyxovirus invasion. Trends Microbiol. **14:**243–246.
22. **Scheid, A., and P. W. Choppin.** 1974. Identification of biological activities of paramyxovirus glycoproteins. Activation of cell fusion, hemolysis, and infectivity of proteolytic cleavage of an inactive precursor protein of Sendai virus. Virology **57:**475–490.
23. **Starr-Spires, L. D., and R. G. Collman.** 2002. HIV-1 entry and entry inhibitors as therapeutic agents. Clin. Lab. Med. **22:**681–701.
24. **Still, W. C., A. Tempczyk, R. C. Hawley, and T. Hendrickson.** 1990. Semianalytical treatment of solvation for molecular mechanics and dynamics. J. Am. Chem. Soc. **112:**6127–6129.
25. **Sun, A., A. Prussia, W. Zhan, E. E. Murray, J. Doyle, L. T. Cheng, J. J. Yoon, E. V. Radchenko, V. A. Palyulin, R. W. Compans, D. C. Liotta, R. K. Plemper, and J. P. Snyder.** 2006. Nonpeptide inhibitors of measles virus entry. J. Med. Chem. **49:**5080–5092.
26. **Sutter, G., M. Ohlmann, and V. Erfle.** 1995. Non-replicating vaccinia vector efficiently expresses bacteriophage T7 RNA polymerase. FEBS Lett. **371:**9–12.
27. **Wolfson, L. J., P. M. Stebel, M. Gacic-Dobo, E. J. Hoekstra, J. W. McFarland, and B. S. Hersh.** 2007. Has the 2005 measles mortality reduction goal been achieved? A natural history modelling study. Lancet **369:**191–200.
28. **Yin, H. S., X. Wen, R. G. Paterson, R. A. Lamb, and T. S. Jardetzky.** 2006. Structure of the parainfluenza virus 5 F protein in its metastable, prefusion conformation. Nature **439:**38–44.